ChemPubSoc Europe

DOI: 10.1002/slct.201601118

Chemistry SELECT Full Papers

Electro, Physical & Theoretical Chemistry

Role of Hydrogen Bond in the Solvation Behavior of the Binary Mixtures Containing Fluorocarbon Alcohol Molecules and Chloroform: An Experimental and Theoretical Study

Biswajit Biswas[+], Saptarsi Mondal[+], and Prashant C. Singh*[a]

Fluorocarbon containing alcohol molecules are important due to their unusual but important physicochemical properties. We have investigated solvatochromic as well as hydrogen bond behavior of weakly interacting binary mixtures of chloroform ($CHCl_3$) with the fluorocarbon containing alcohols namely, 2-fluoroethanol (MFE) and 2,2,2-trifluoroethanol (TFE) as well as compared them with ethanol (ETH)-$CHCl_3$ binary mixture. UV-Vis study depicts that the particular composition ($\chi_{ETH} \sim 0.6$) of the binary mixtures of $CHCl_3$ with ETH and MFE solvate probes more efficiently as compared to the respective counterparts, whereas, the probes are preferably solvated by the TFE as compared to solvent mixtures in the case of TFE-$CHCl_3$ binary mixture. NMR, IR as well as theoretical calculations establish that $CHCl_3$ forms the C–H…O hydrogen bonded clusters with ETH and MFE whereas TFE-$CHCl_3$ binary mixture are connected predominantly through C–H…F hydrogen bond. The dipole of probe molecules perturbs the weaker C–H…F hydrogen bond present in the TFE-$CHCl_3$ binary mixture resulting in the preferential solvation by the TFE, whereas, the comparatively stronger C–H…O hydrogen bonded species is preserved in the binary mixtures of $CHCl_3$ with ETH and MFE which leads to the favorable solvation by the binary mixtures of $CHCl_3$ with ETH and MFE. Further, analytical solvent exchange models have been used to substantiate the solvation behavior of the probe molecules in the $CHCl_3$ binary mixtures with ETH and TFE.

Introduction

Solvent mixtures are important systems which are being regularly used in many chemical, physical, biochemical as well as industrial processes such as chromatography, cell suspension, soil suspension and nano catalysis. The physical properties of solvent mixtures are often different from their constituents due to the presence of micro-heterogeneous environment in the solvent mixtures. The behavior of solvent mixtures towards any solute depends on the nature and extent of the solute-solvent interaction originating in the immediate vicinity of the solute molecules.[1–4] The behavior of any solute molecule in solvent mixtures depends on their interaction with its constituents either in a specific or non-specific way.[5–8] The solute molecule may be solvated predominantly by one of the solvent of the mixture through specific or non-specific interaction, known as preferential solvation.[3,9] In other cases, both constituents of the solvent mixture can solvate a probe molecule as a different entity which provides a completely different solvation environment around the solute molecule causing to show a significant change of a particular property (solvation in the present study) from its bulk counterparts and this effect is known as synergetic effect.[10] The experimental and theoretical tools have been used in a great deal to understand the preferential solvation as well as synergetic behavior of the solvent mixtures.[5,7,8,10–22] Several different spectroscopic techniques such as UV-Vis,[8,11] NMR,[23,24] vibrational spectroscopy,[25,26] solvation dynamics,[27] two dimensional infrared techniques[20,21] have been used to understand the behavior of solvent mixtures as these techniques have the capability to provide the quantitative information about the solute-solvent interaction as well as hydrogen bond network present in solvent mixtures. Molecular dynamics simulations (MD) have further enlightened the understanding of the various reasons responsible for the non-ideal behavior of the solvent mixtures.[5,22]

Solvent mixtures containing amphiphilic molecules such as alcohols, dimethyl sulfoxide, acetone, and glycerol have drawn huge attention as these molecules possess both hydrophilic and hydrophobic groups.[28–30] Hydrophilic group of amphiphilic molecules may interact with the water molecules through hydrogen bonds, whereas, the hydrophobic part can induce ordering by the cooperative hydrophobic interaction. Solvent mixtures containing amphiphilic molecules are found to show non-ideal behavior for many different physical properties such as viscosity, surface tension, volume as the hydrophilic and hydrophobic effect perturbed the hydrogen bonding network extensively in the solvent mixture. Alcohol containing solvent mixtures is important systems owing to their implication in

[a] B. Biswas,[+] S. Mondal,[+] Dr. P. C. Singh
Department of Spectroscopy
Indian Association for the Cultivation of Science
Kolkata 700032, India
Phone: +91 33 2473 4971
E-mail: sppcs@iacs.res.in

[+] Both authors share equal contribution.

Supporting information for this article is available on the WWW under http://dx.doi.org/10.1002/slct.201600118

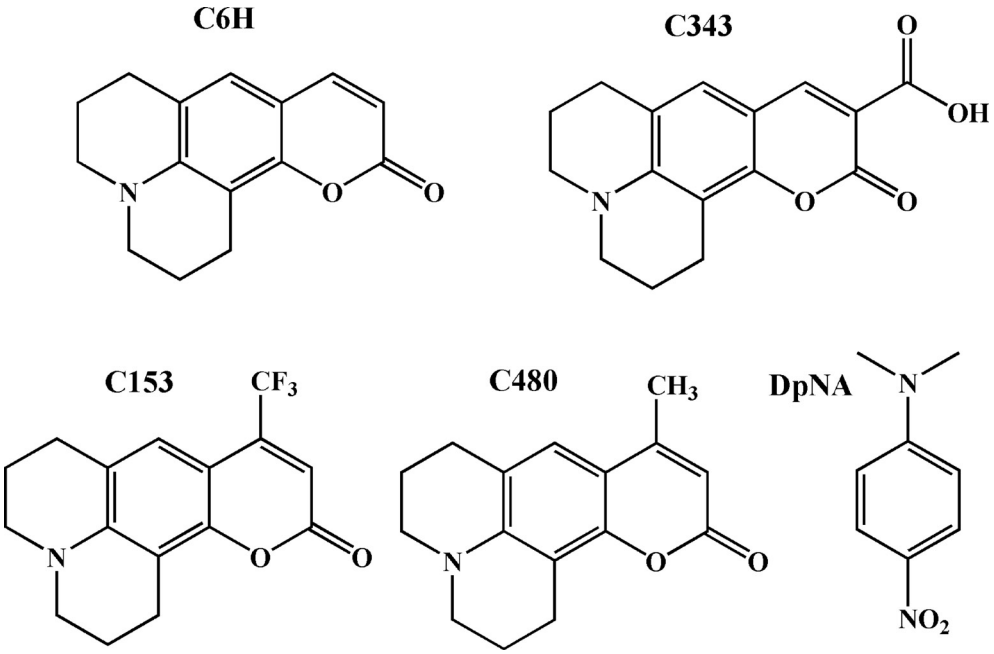

Figure 1. Chemical structures of solvatochromic probes.

many biological and chemical processes. Aqueous ethanol (ETH) solution is the most explored system through various experimental as well as theoretical studies and has been found to show non-ideal behavior. Partial molar volumes, dielectric, differential scanning calorimetric, X-ray diffraction as well as spectroscopic studies have shown that ETH-water mixture shows non-monotonic behavior around the ~ 0.2 mole fraction of ethanol (χ_{ETH}).[29] Several MD simulations on the ETH-water mixture have indicated the structural heterogeneity of solvent mixture as a probable reason for their non-ideal behavior.[30,31]

Fluorocarbon substituted alcohols are important due to the unusual but important physicochemical properties of the fluorocarbon group and have shown importance in several applications such as protein engineering, fire retardants, anesthetics, and organic synthesis.[32–34] 2,2,2-Trifluoroethanol (TFE) is one of the most important fluorocarbon containing alcohols due to its diverse application in the field of biology. One of the most interesting observations related to the TFE is that the aqueous solution of TFE enhances the stability of proteins as compared to the bulk water and ETH-water.[33,34] The C–F bond of TFE is the main reason responsible for the difference in the behavior of TFE as compared to ETH. Indeed, the C–F bond of fluorocarbons is longer as well as stronger compared to C–H. C–F bond is less polarizable as compared to C–H due to the high electronegativity of the fluorine. The dipole moment of the C–F bond is directionally opposite to C–H as well as a C–F bond is more stable as compared to the C–H bond by 14 kcal/mol. The higher stability as well as dipole moment of C–F bond make perfluorinated molecules extreme hydrophobic, inert, and less polarizable which imparts them with unusual phase segregating properties.

The solvent mixtures of alcohols with chloroform ($CHCl_3$) are important systems due to their manifold applications. $CHCl_3$ forms azeotrope mixtures with alcohols where the aggregation of the alcohols is perturbed weakly by the C–H group of alcohols. The solvation properties of the probe in the solvent mixtures of the $CHCl_3$ with ETH and methanol have been studied. However, our knowledge about the solvation as well as the hydrogen bond interaction between the constituents of solvent mixtures containing fluorocarbon alcohol molecules is sparse. As we have discussed earlier that C–F bond is extreme hydrophobic, inert as compared to the C–H, hence, it will be interesting to understand the role of C–F group in the solvation as well as hydrogen bond properties of solvent mixtures of fluorocarbon containing alcohols with the $CHCl_3$. In this paper, we have studied the solvent mixtures of ETH, 2-fluoroethanol (MFE) and TFE with $CHCl_3$ using several spectroscopic techniques such as UV-Vis, NMR, and IR techniques along with density function theory (DFT) calculations. We have found that binary mixture of $CHCl_3$ with ETH and MFE shows synergetic effect, whereas, the binary mixture of $CHCl_3$ with TFE shows the preferential solvation. NMR, IR studies along with the DFT calculations depict that ETH and MFE interact with $CHCl_3$ mainly via the C–H…O hydrogen bond, whereas, TFE interacts with $CHCl_3$ predominantly through weak C–H…F hydrogen bond. The weak C–H…F hydrogen bond present in the binary mixture of $CHCl_3$ with TFE gets perturbed by the dipole moment of the solute causing to the preferential solvation behavior.

Results and Discussion

UV-Vis Absorption

UV-Vis spectra of a series of solvatochromic dyes of different nature (structures are given in Figure 1) were measured in the binary mixtures of $CHCl_3$ with ETH, MFE and TFE respectively, in order to characterize the properties of different chloroform-

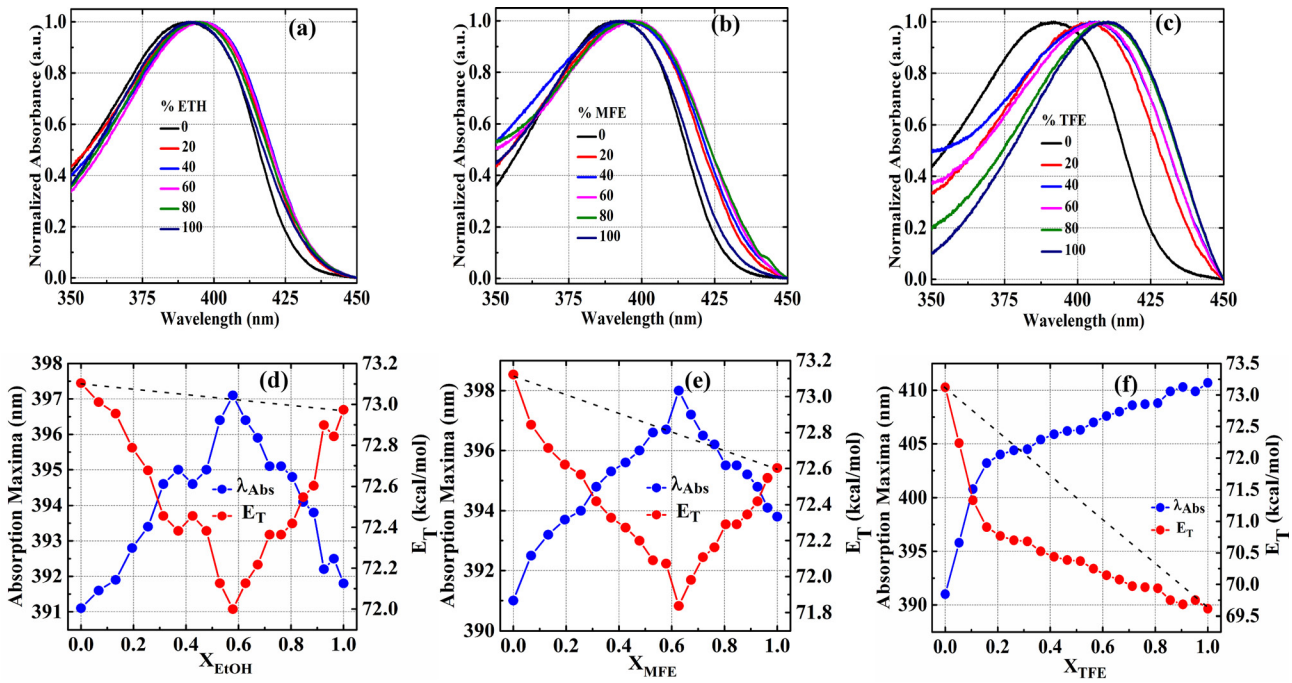

Figure 2. Normalized steady sate UV-Vis spectra of the C6H at different compositions of the binary mixtures of $CHCl_3$ with ETH (a), MFE (b) and TFE(c), respectively. The variation of the absorption maxima ($\lambda_{max,}$ blue line) of the UV-Vis as well as the molar transition energy (E_T, red line) with respect to the mole fraction of alcohols for the binary mixtures of $CHCl_3$ with ETH (d), MFE (e) and TFE(f), respectively. Black dotted line shows the ideal behavior of binary mixtures.

alcohol mixtures. The dye concentration was kept to 5 μM in order to rule out the possibility of the interaction between the solute molecules. Figure 2 shows the UV-Vis spectra of C6H in different alcohols-chloroform binary mixtures (a-c) along with the variation of the peak maxima of UV-vis spectrum (λ_{max}) with respect to the mole fraction of alcohols in alcohol-$CHCl_3$ binary mixture (d-f, blue line). The λ_{max} of C6H in pure $CHCl_3$, ETH, MFE and TFE were found to be 391.1, 391.8, 393.8 and 410.7 nm, respectively. With increasing mole fraction of ETH, the λ_{max} of C6H was found to be shifting towards longer wavelength and after certain mole fraction of ETH, it decreases towards shorter wavelength. The maximum value of λ_{max} of C6H has been found for the χ_{ETH} of 0.57 (Figure 2d, blue line) in ETH-$CHCl_3$ binary mixture. This clearly suggests that the ETH-$CHCl_3$ mixture could solvate C6H more efficiently with respect to pure $CHCl_3$ or ETH. Similar observation was found for the MFE-$CHCl_3$ binary mixture where the maximum value of λ_{max} of C6H has been found for the χ_{MFE} of 0.62 (Figure 2e, blue line). The $CHCl_3$ mixture with ETH and MFE solvate to the solute more as compared to the pure mixtures suggesting that the $CHCl_3$ mixtures of ETH and MFE interacts with solute in completely different manner as compared to their pure solvents which has been defined as the synergetic effect. However, the λ_{max} keeps on shifting towards the higher wavelength with the increase of χ_{TFE} (Figure 2f, blue line) for the TFE-$CHCl_3$ binary mixture in contrast to the binary mixtures of chloroform with ETH and MFE. C6H dye molecules were found to be preferentially solvated by TFE as compared to $CHCl_3$ as well as their binary mixture, in contrast to the behavior of binary mixtures of $CHCl_3$ with ETH and MFE

We have calculated the molar transition energy (E_T) for different alcohol-$CHCl_3$ mixtures in order to correlate the observed change in UV-Vis spectrum of C6H with a physical quantity. The molar transition energy E_T (kcal/mol) is calculated by equation 1 which correlates the λ_{max} with E_T.

$$E_T\ (\text{kcal/mol}) = hcN_A/\ \lambda_{max}\ (\text{nm}) = 28591.5/\ \lambda_{max}\ (\text{nm}) \qquad (1)$$

$$E_{Tideal}\ (\text{kcal/mol}) = X_1E_{T(1)}\ +\ X_2E_{T(2)} \qquad (2)$$

Where h, c and N_A are Planck's constant, the velocity of light and Avogadro's number, respectively. The change in the values of E_T as a function of mole fraction of alcohols is presented in Figure 2(d-f, red line) for the C6H dye. For an ideal case, for all proportion of binary mixtures, E_T value of the solvent mixtures will follow equation 2. $E_{T(i)}$ represent values of molar transition energy of a dye or indicator solute in pure solvent 1 and 2, and X_i are the mole fractions of solvent 1 and 2. Hence, for the ideal mixtures, E_T will be linear in the entire mole fraction range of binary solvent mixture as shown by the dotted black line in Figure 2 (d-f). The variation of E_T for all the mixtures is not linear (Figure 2d–f, red line) depicting that the binary mixtures of $CHCl_3$ with different alcohols are non-ideal systems.

In general, the variation from the ideal behavior could be either due to solute–solvent or solvent-solvent interactions. The $CHCl_3$ mixture with ETH and MFE shows the synergetic behavior, whereas, the TFE-$CHCl_3$ depicts the preferential solvation for the C6H dyes. The different behavior of the TFE-$CHCl_3$ binary mixture as compared to the binary mixtures of

$CHCl_3$ with ETH and MFE could be either due to the probe molecule or the difference in the hydrogen bond between the constituents present in the binary mixtures. Further, we have studied different kinds of probe molecules such as coumarin 480 (C480), coumarin 153 (C153), coumarin 343(C343) and N, N Dimethyl-*p*-nitroaniline (DpNA) in different alcohol-$CHCl_3$ binary mixtures in order to differentiate the role of probe and solvent hydrogen bond for the different behavior of the binary mixtures of alcohols with $CHCl_3$. Amongst these dyes, C480 and C153 dyes are hydrophobic, C343 is hydrophilic and DpNA is hydrogen bond acceptor molecule, respectively. The variation of λ_{max} as well as E_T for all the dyes in different alcohol-$CHCl_3$ binary mixtures is shown in the Figure S1. The trend of λ_{max} values of all dyes in ETH-$CHCl_3$ and MFE-$CHCl_3$ binary mixtures are higher as compared to the pure solvent indicating that the synergetic effect is prominent in these cases. However, λ_{max} values of all the dyes for the TFE-$CHCl_3$ mixture are high for the pure TFE as compared to their binary mixture suggesting the preferential solvation of the dye by the respective solvent. This study clearly shows that the hydrogen bond in TFE-$CHCl_3$ solvent mixture is distinctly different from solvent mixtures of $CHCl_3$ with ETH and MFE due to which synergetic behavior was found for the $CHCl_3$ binary mixtures with ETH and MFE, whereas, the TFE-$CHCl_3$ solvent mixture shows the preferential solvation.

NMR and IR studies

In binary mixtures, solvent molecules interact with each other generally through hydrogen bonding and hence, as the proportion of either of the counterparts is changed, the local electronic cloud around the hydrogen bonded atoms of each solvent changes which can be directly realized by the change in chemical shifts (δ) of that particular group obtained from NMR spectra. Proton magnetic resonance (^{1}H-NMR) measurements for CH group of $CHCl_3$ as well as OH of the alcohols have been performed using 500 MHZ NMR spectrometer in order to ensure the nature of hydrogen bond between the solvent constituents of alcohols-$CHCl_3$ binary mixtures (Figure S2). Figure 3 shows the variation of δ values of CH proton of $CHCl_3$ (a) as well as OH protons of alcohols (b) for the different composition of the binary mixtures of $CHCl_3$ with alcohols. In case of ETH-$CHCl_3$ binary mixture, the δ value of the proton of $CHCl_3$ shifts towards upfield with increasing χ_{CHCl3} and at the same time, the δ value of the OH proton of ETH shifts towards downfield with increasing χ_{ETH} (black line in Figures 3a and 3b respectively). This observation is consistent with the earlier NMR study for the $CHCl_3$ binary mixture with methanol.[11] The trend of the δ values of $CHCl_3$ proton and alcoholic OH proton for the MFE-$CHCl_3$ binary mixture is similar to ETH-$CHCl_3$ except that the change in the δ value of $CHCl_3$ proton is less in the case of MFE-$CHCl_3$.[11] The observed NMR data for the $CHCl_3$ mixture with ETH and MFE indicates that self aggregation of the ETH/MFE molecules minimized with the increase of the $CHCl_3$ and the hydrogen bonding interaction initiates between the $CHCl_3$ and ETH/MFE. Surprisingly, for the case of TFE-$CHCl_3$ binary mixture, the change in the δ value of the $CHCl_3$ proton is very less as compared to MFE and ETH, whereas, change in the δ value of OH proton of TFE is qualitatively similar to the MFE and ETH. The trend of δ values for TFE-$CHCl_3$ mixture depicts that $CHCl_3$ interacts with TFE in a markedly different way as compared to MFE and ETH.

Further, we have modeled the proton chemical shift of C–H group of $CHCl_3$ as well as OH of alcohols to know the interaction between $CHCl_3$ and different alcohols in their respective solvent mixtures. The observed proton chemical shift data (δ_{obs}) for the OH group of alcohols can be represented as a linear combination of the chemical shift of the self associated alcohol molecules (δ_{AA}) and the chemical shift of OH proton of alcohols hydrogen bonded to the $CHCl_3$ (δ_{AC}).

$$\delta_{Obs} = \frac{\chi_{AA}}{\chi_A} \times \delta_{AA} \times \frac{\chi_{AC}}{\chi_A} \times \delta_{AC} \quad (3)$$

Where χ_{AA}, χ_{AC} and χ_A are the mole fraction of the alcohols in the self aggregated form, mole fraction of alcohol bound to $CHCl_3$ and total mole fraction of the alcohol in the mixtures ($\chi_{A=}\ \chi_{AA} + \chi_{AC}$), respectively. Experimentally observed δ value for the pure alcohol represents the chemical shift for self aggregated (δ_{AA}) alcohol molecules. However, the chemical shift for δ_{AC} can not be obtained directly. In order to obtained the δ_{AC}, equation 3 has been rewritten as,

$$\delta_{Obs} = \delta_{Ac} + \frac{\chi_{AA}}{\chi_A} \times (\delta_{AA} - \delta_{AC}) \quad (4)$$

χ_{AA} can be obtained by fitting the observed proton chemical shift of OH group of alcohols with respect to χ_A by the normalized function as shown in equation (5). Once we obtained the χ_{AA}, χ_{AC} can be obtained by using the relation, $\chi_A = \chi_{AA} + \chi_{AC}$

$$\frac{\chi_{AA}}{\chi_A} = \frac{y_0 + a_1 \times e^{(-\chi_A/t_1)} + a_2 \times e^{(-\chi_A/t_2)}}{y_0 + a_1 \times e^{(-1/t_1)} + a_2 \times e^{(-1/t_2)}} \quad (5)$$

Similarly, the mole fraction of the $CHCl_3$ bound to the alcohols (χ_{CA}) in their mixtures can be obtained by equations (6) and (7)

$$\delta_{Obs} = \frac{\chi_{CC}}{\chi_C} \times \delta_{CC} + \frac{\chi_{CA}}{\chi_C} \times \delta_{CA} \quad (6)$$

$$\delta_{Obs} = \delta_{CA} \times \frac{\chi_{CC}}{\chi_C} \times (\delta_{CC} - \delta_{CA}) \quad (7)$$

Where δ_{cc}, δ_{CA} represents the mole fraction of self aggregated $CHCl_3$ and $CHCl_3$ hydrogen bonded to alcohols in their respective mixtures. χ_{CC} and χ_C are the mole fraction of the $CHCl_3$ in the self aggregated form and total mole fraction of the $CHCl_3$ in the respective mixtures ($\chi_{C=}\ \chi_{CC} + \chi_{CA}$), respectively. We have fit the experimentally observed proton chemical shift data for OH group of alcohols as well as CH group of chloroform to obtain the value of χ_{AC} and χ_{AC} in their respective mixtures. The fitting of NMR data for ETOH- $CHCl_3$ mixture has been shown in the Figure 4 where as the fitting for the $CHCl_3$ mixtures with MFE and TFE are depicted in the supporting

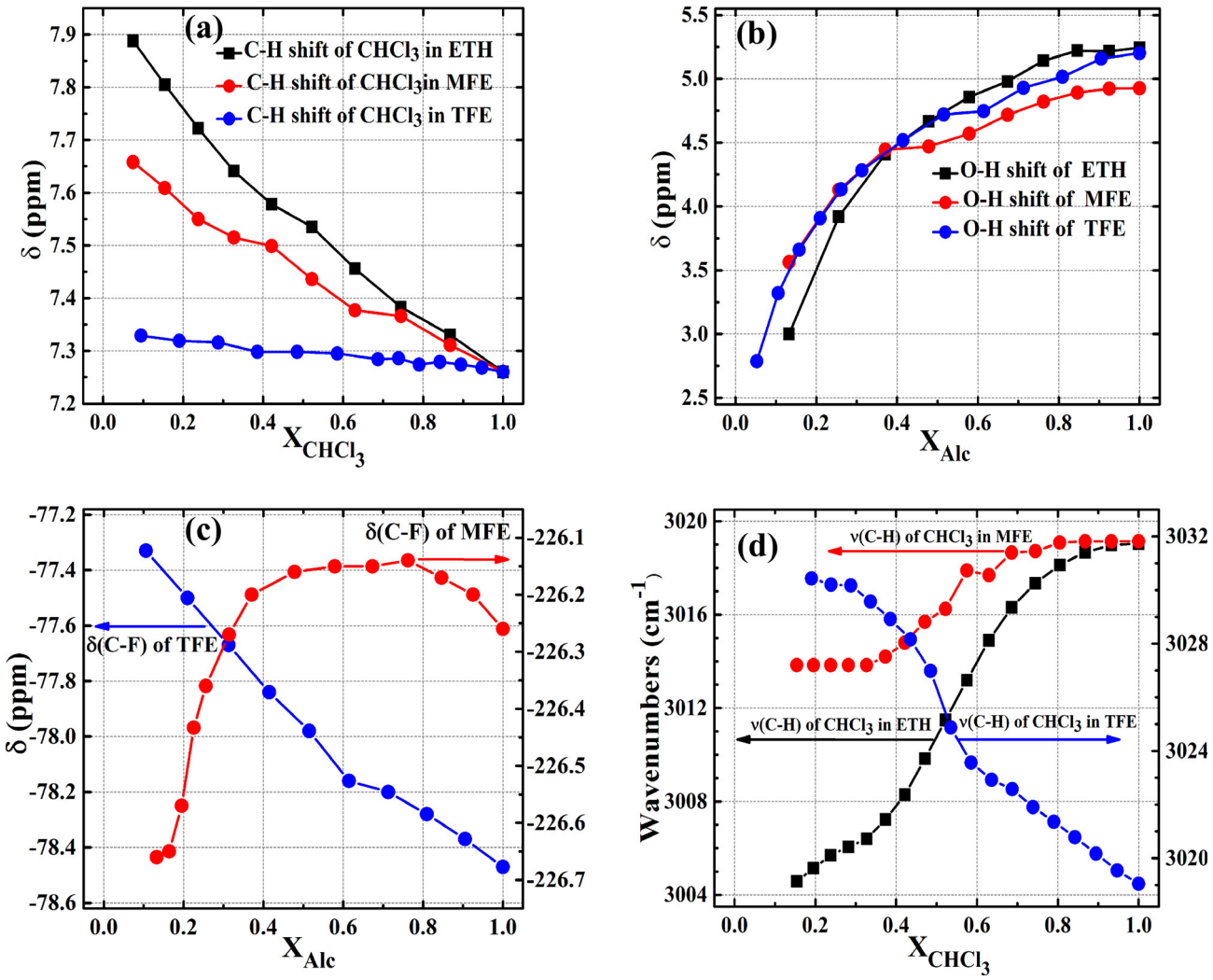

Figure 3. The change in chemical shift (δ) for the C–H group of $CHCl_3$ (a) as well as O–H group of alcohols in the different compositions of the binary mixtures of $CHCl_3$ with ETH (black line), MFE (red line) and TFE (blue line), respectively. The change in δ for the C–F group of MFE (c, red line) as well as TFE(c, blue line) for the different compositions of the binary mixtures of $CHCl_3$ with MFE and TFE, respectively. The change in the C–H stretching frequency (d) of $CHCl_3$ in the different compositions of the binary mixtures of $CHCl_3$ with ETH (black line), MFE (red line) and TFE (blue line), respectively.

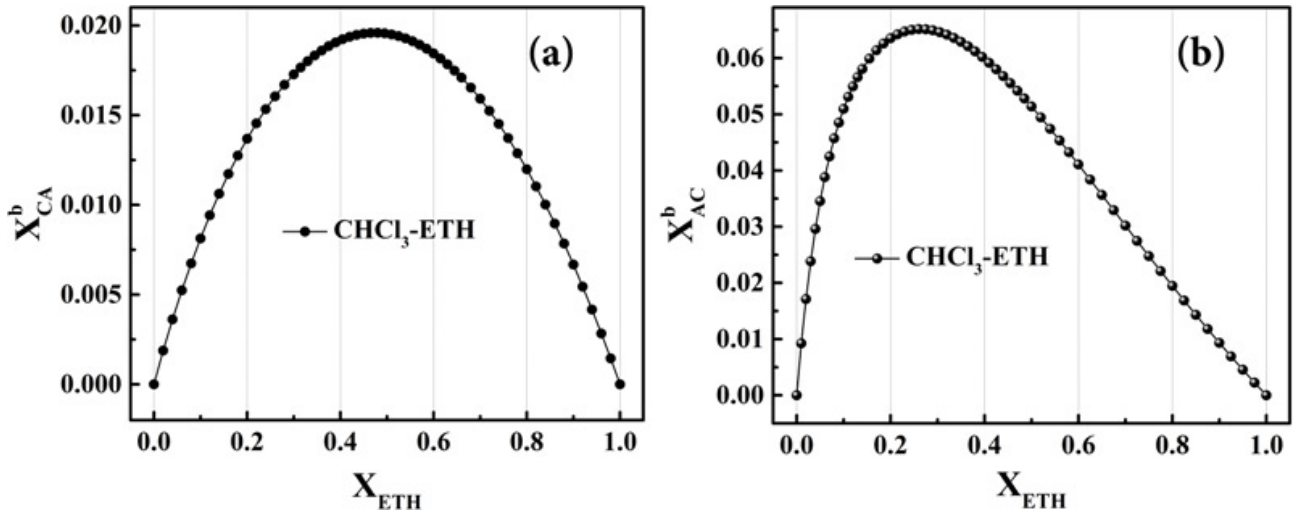

Figure 4. Plot of mole fraction of $CHCl_3$ bonded to ETH (χ_{CA}) (a) as well as ETH bonded to $CHCl_3$ (χ_{AC}) (b) against χ_{ETH} in the case of $CHCl_3$-ETH binary mixture.

information (Figure S3). The fitted data in Figure 4 shows that the maximum fraction of ETH bonded to $CHCl_3$ appears at χ_{ETH} of ~0.25 whereas maximum for the $CHCl_3$ bonded to ETH comes at χ_{ETH} of ~0.50 which indicates that probably two $CHCl_3$ molecules interact with one ETH in the mixture. We have found similar trend in the case of $CHCl_3$ mixtures with MFE and TFE suggesting that the $CHCl_3$ binds with all alcohols in the same stoichiometric ratio. However, the trend of chemical shift of the proton NMR of C–H group of $CHCl_3$ indicates that the mode of interactions of $CHCl_3$ with TFE is different as compared to ETH and MFE.

To understand the role of fluorine in the hydrogen bonding of the $CHCl_3$ with MFE and TFE, we have measured the ^{19}F NMR spectra for these two binary mixtures and the change in the δ values with respect to the increase of alcohol concentration of the mixtures has been depicted in Figure 3c. For TFE-$CHCl_3$ binary mixture, the δ value shifted towards the up-field with increasing χ_{TFE} whereas, the δ value for MFE-$CHCl_3$ mixture moves towards the downfield with the increase of the MFE up to the χ_{MFE} ~0.52 and then becomes almost constant. The change in the δ values for the MFE is smaller as compared to the TFE which shows that interaction of fluorine in the case of MFE is weaker as compared to TFE. Overall change in the δ values for the ^{19}F NMR spectra indicates that the interaction of fluorine of TFE with $CHCl_3$ is different from MFE.

Further, to obtain deeper insights into the nature of interaction of $CHCl_3$ mixtures with alcohols, we have measured the IR spectra of the C–H stretching frequency of the $CHCl_3$ as the donor stretching frequency is very sensitive to hydrogen bonding environment[35–37] and the results are depicted in Figures 3d and S4. The C–H stretching of $CHCl_3$ decreases with the increase in the amount of alcohol in ETH and MFE mixtures of $CHCl_3$ whereas; the change of C–H stretching of $CHCl_3$ in TFE-$CHCl_3$ mixture is opposite and increases with the increase in the amount of alcohol. It is well known that the donor stretching frequency in the hydrogen bonded complexes generally shifts towards the red end. The IR as well as NMR data for the $CHCl_3$ binary mixtures with ETH and MFE combinedly infer that the C–H group of $CHCl_3$ act as donor and form hydrogen bond with ETH and MFE. ETH has only oxygen atom as hydrogen bonding acceptor site, hence, C-$H_{(CHCl3)}$…$O_{(ETH)}$ type of hydrogen bonding is taking place with the increase of ETH mole fraction. The different trend of C–H stretching frequency as well as the chemical shift of the C–H group of the $CHCl_3$ in TFE suggests that the C–H of $CHCl_3$ is not interacting with the oxygen of the TFE and probably interacting with the fluorine of TFE through C-$H_{(CHCl3)}$…$F_{(TFE)}$ hydrogen bond. Indeed, several experimental and theoretical studies have shown that donor stretching frequency gets blue shifted when it interacts with the fluorine group of the acceptor molecules.[38] Both, fluorine and oxygen of MFE can act as acceptors and interact with the C–H group of $CHCl_3$; however, the amount of red shift in the C–H stretching as well as change in the chemical shift of the C–H group of the $CHCl_3$ in the MFE-$CHCl_3$ binary mixture is similar but less as compared to ETH-$CHCl_3$ binary mixture indicating the possibility of the formation of both C-$H_{(CHCl3)}$…$O_{(MFE)}$ as well as C-$H_{(CHCl3)}$…$F_{(MFE)}$ type of hydrogen bonding for the MFE-$CHCl_3$ binary mixture, of which C-$H_{(CHCl3)}$…$O_{(MFE)}$ interaction is the most prominent.

Theoretical calculation:

To obtain further insights about the intermolecular interaction between the alcohols and $CHCl_3$ in their respective mixtures, we have performed the optimization and frequency calculation for their microhydrated clusters using the polarization continuum model incorporated in the Gaussian 09 suit of program. We have optimized the dimer of alcohols and chloroform in the alcohol and chloroform solvent respectively as the representative structure of pure alcohol and chloroform solution assuming that alcohols will form high order of clusters in pure alcohol and same is true for chloroform in pure chloroform solution. Alcohol-$CHCl_3$ as well as (alcohol)$_2$-$CHCl_3$ have been optimized in the alcohol medium representing the structure of mixture of alcohol-$CHCl_3$ in alcohol region, whereas, alcohol-$CHCl_3$ as well as alcohol-$(CHCl_3)_2$ have been optimized in chloroform representing the structure of mixture of alcohol-$CHCl_3$ in chloroform region.

Figure 5 shows the optimized structures of ETH, MFE and TFE complexes with $CHCl_3$ in the respective alcohol medium at the B3LYP/6-31G (d) level of theory. It can be seen that $CHCl_3$ interacts with ETH via C–H…O hydrogen bonding, whereas, $CHCl_3$ interacts with MFE and TFE through C–H…O as well as C–H…F hydrogen bonds. All alcohols associate within themselves via O–H…O hydrogen bond. The stabilization energy (ΔE) of the different structures of alcohol-$CHCl_3$ complexes depict that ΔE values for the C–H….O hydrogen bonded complexes of TFE with $CHCl_3$ is slightly less as compared to that of ETH and MFE complexes with $CHCl_3$. In the case of MFE and TFE, the O–H…O interaction in the dimer has similar stabilization energy, while the structures with C–H…O, O–H…O and C–H…F, O–H…O interactions have different stabilization energies which is probably due to the induction effect of the fluorine which reduces the electron density on the oxygen atom of MFE and TFE. The stabilization energy of the C–H…F hydrogen bonded complexes of MFE and TFE with $CHCl_3$ is very close to their C–H…O hydrogen bonded structures indicating the possibility of C–H…F hydrogen bonded complexes along with the C–H…O hydrogen bonded complexes for MFE and TFE.

In order to have an in depth understanding of the structures of alcohol-$CHCl_3$ mixture responsible for the experimental NMR and IR data, we have calculated the chemical shift of the proton of C–H group of $CHCl_3$ and O–H group of alcohols along with the C–H stretching frequency of $CHCl_3$ for the different structures at the B3LYP/6-31G (d) level of theory. It can be seen that the calculated proton NMR shift of the OH group of alcohols decreases with the addition of the $CHCl_3$ irrespective of the nature of the interaction, similar to the experimental data. The calculated chemical shift of the proton of the C–H group of $CHCl_3$ increases with the addition of alcohols as compared to the pure $CHCl_3$ which is in line to the experimental observation. The experimental value for the proton chemical shift of the C–H group of $CHCl_3$ increases

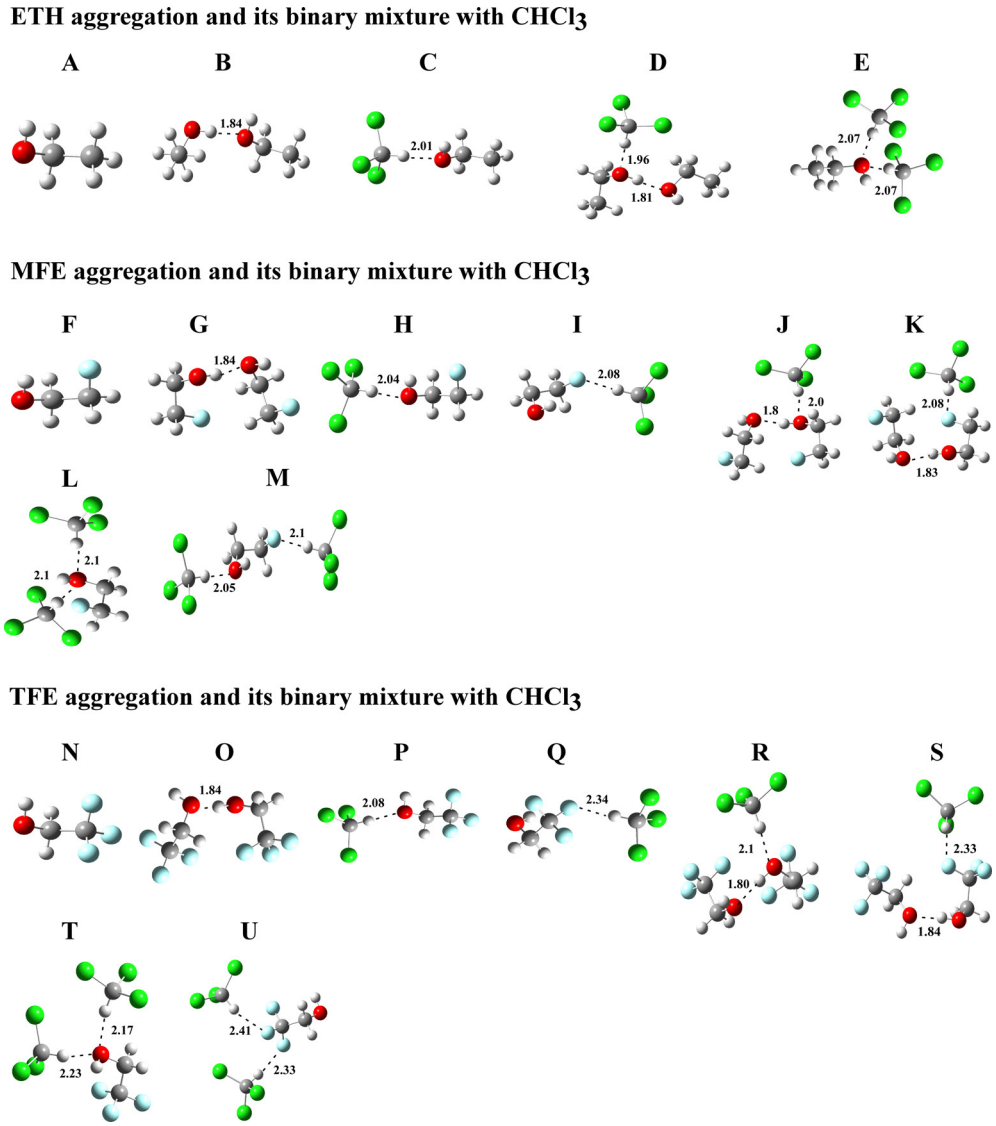

Figure 5. The optimized structures of the $CHCl_3$ complexes with ETH (ETH solvent medium), MFE (MFE solvent medium) and TFE (TFE solvent medium), respectively at the B3LYP/6-31 g (d) level of calculation using the polarized continuum model. The distances (Å) are shown in the black line. Oxygen, carbon, hydrogen, chlorine, and fluorine are shown in the red, grey, white, green and light blue colors, respectively.

maximally for the ETH-$CHCl_3$ complexes (from 7.15 ppm to 7.9 ppm) whereas, in the case of TFE, it increases marginally (from 7.15 ppm to 7.32 ppm). It can be seen that the calculated proton chemical shift of the C–H group of $CHCl_3$ for the C–H…O hydrogen bonded complexes are higher (~8.4 ppm) as compared to chloroform monomer (~7.40 ppm) whereas, the chemical shift for the C–H….F hydrogen bonded complexes (~7.45 ppm) are similar to the chloroform monomer (~7.40 ppm) .The vibrational frequency of the C–H stretching of the $CHCl_3$ for the different structures of alcohol-$CHCl_3$ complexes shows that the C–H…O hydrogen bonded complexes show the red shift, whereas, a blue shift in the C–H stretching frequency of $CHCl_3$ has been obtained for the C–H…F hydrogen bonded complexes as compared to the $CHCl_3$ monomer. It is true that the absolute value of the change in frequency as well as the chemical shift obtained from the theoretical calculation does not perfectly match with the experimental data as it has been calculated on the model system to have qualitative information about the nature of interaction present in the different alcohols-$CHCl_3$ mixtures. The trend of experimental and theoretical data of the proton chemical shift of the C–H group of $CHCl_3$ along with the vibrational frequency data clearly elicits that $CHCl_3$ interacts with ETH via C–H…O hydrogen bonds, whereas, $CHCl_3$ interact with the TFE through C–H…F hydrogen bonded species. TFE have CF_3 group which is lipophilic and prefer to interact with the CF_3 group of other TFE molecules. MD simulations have shown that the bulk TFE forms micelle like structures in which CF_3 groups of TFE are outside interacting with each other, whereas, the OH groups are inside forming O–H…O hydrogen bond with each other.[39] On addition of $CHCl_3$, the lipophilic character of CF_3 group probably does not allow them to go inside and hence, maximum of C–H group interacts with the fluorine of TFE through C–H….F hydrogen bond. Indeed, it has been shown through MD simulations that the oxygen atom of TFE has only three water molecules in comparison to twenty water molecules near the CF_3 group of TFE indicating that water forms cage like structure near the CF_3 group of TFE.[32,40] The case of

Table 1. The stabilization energy (ΔE, kcal/mol), change in the stretching frequency of the C–H group of $CHCl_3$ (cm^{-1}) and the chemical shift of the OH of the alcohols and C–H of the $CHCl_3$ in the complexes of $CHCl_3$ with ETH, MFE and TFE calculated at the B3LYP/6-31G (d) level of theory. Polarization continuum model has been used in order to incorporate the effect of different solvents in the calculation.

System ETH	Interaction type	Name(solvent)	ΔE	$\Delta\nu_{(C\text{-}H)\ chl}$	$\delta_{H\ (O\text{-}H)alc}$	$\delta_{H\ (C\text{-}H)chl}$
ETH		A(ETH)			4.27	
$(ETH)_2$	O–H…O	B(ETH)	-6.6		8.41, 4.91	
$(ETH)_2$-$CHCl_3$	C–H…O, O–H…O	C(ETH)	-11.4	-147	7.91, 4.84	9.09
ETH-$CHCl_3$	C–H…O	D(ETH)	-4.4	-105	4.78	8.80
ETH-$CHCl_3$	C–H…O	D ($CHCl_3$)	-4.1	-89	4.62	8.77
ETH-$(CHCl_3)_2$	C–H…O	E ($CHCl_3$)	-7.2	-60, −68	5.24	8.58, 8.59
$(CHCl_3)_2$		$CHCl_3$	-0.3	4		7.43, 7.44
$CHCl_3$		$CHCl_3$				7.40
MFE						
MFE		F(MFE)			5.42	
$(MFE)_2$	O–H…O	G(MFE)	-7.9		8.95, 6.02	
$(MFE)_2$-$CHCl_3$	C–H…O, O–H…O	H(MFE)	-12.7	-114	8.72, 5.75	8.75
$(MFE)_2$-$CHCl_3$	C–H…F, O–H…O	I(MFE)	-10.2	-2	8.38, 5.94	7.62
MFE-$CHCl_3$	C–H…O	J(MFE)	-3.9	-87	5.90	8.70
MFE-$CHCl_3$	C–H…F	K(MFE)	-3.2	+5	5.51	7.72
MFE-$CHCl_3$	C–H…O	J($CHCl_3$)	-4.3	-73	5.83	7.68
MFE-$CHCl_3$	C–H…F	K($CHCl_3$)	-3.5	+13	5.43	8.73
MFE-$(CHCl_3)_2$	C–H…O	L($CHCl_3$)	-7.3	-48, −57	5.28	8.42, 8.47
MFE-$(CHCl_3)_2$	C–H…F, C–H…O	M($CHCl_3$)	-5.5	+11, −71	5.86	7.67, 8.61
TFE						
TFE		N(TFE)			5.18	
$(TFE)_2$	O–H…O	O (TFE)	-7.6		8.56, 8.47	
$(TFE)_2$-$CHCl_3$	C–H…O, O–H…O	P (TFE)	-5.0	-54	5.92, 5.87	8.38
$(TFE)_2$-$CHCl_3$	C–H…F, O–H…O	Q (TFE)	-8.0	+21	8.02, 5.78	7.49
TFE-$CHCl_3$	C–H…O	R(TFE)	-3.2	-56	5.61	8.42
TFE-$CHCl_3$	C–H…F	S (TFE)	-2.1	20	5.30	7.45
TFE-$CHCl_3$	C–H…O	R ($CHCl_3$)	-3.4	-46	5.48	8.37
TFE-$CHCl_3$	C–H…F	S ($CHCl_3$)	-2.2	26	5.16	7.40
TFE-$(CHCl_3)_2$	C–H…O	T ($CHCl_3$)	-4.3	-10, −28	5.84	8.05, 8.24
TFE-$(CHCl_3)_2$	C–H…F	U ($CHCl_3$)	-6.7	26, 25	5.26	7.41, 7.45

MFE-$CHCl_3$ mixture is in between ETH and TFE where the $CHCl_3$ may interact with MFE via both C–H…O and C–H…F hydrogen bonds, however, the experimental data suggests that the major contribution is coming from the C–H…O hydrogen bonded species.

The behavior of any probe molecule in the solvent depends on the strength of the hydrogen bond of the solvent mixture as well as the dipole of the probe molecule. The presence and absence of the synergetic effect in ETH-$CHCl_3$ and TFE-$CHCl_3$ mixtures is due to the difference in the hydrogen bond of $CHCl_3$ with ETH as compared to the TFE. The addition of $CHCl_3$ in ETH disturbs the O–H…O hydrogen bond between the ETH molecule and the formation of C-$H_{(CHCl3)}$…$O_{(ETH)}$ hydrogen bond takes place which is maximum at the χ_{ETH} of 0.57. The hydrogen bonding pattern in the MFE-$CHCl_3$ is similar to ETH except that some of the $CHCl_3$ also forms C-$H_{(CHCl3)}$…F-$C_{(MFE)}$ hydrogen bond with MFE. In case of TFE-$CHCl_3$ mixture, TFE arranges itself to maximize the lipophilic interaction; hence, O–H…O interaction between TFE takes place in such a way that the CF_3 group of TFE comes closer to each other. On addition of $CHCl_3$, the maximum of CF_3 group of TFE interacts with $CHCl_3$ through C-$H_{(CHCl3)}$…F_3-$C_{(TFE)}$ group. The binding energy of the C–H…O hydrogen bonded complexes of ETH and MFE mixture with $CHCl_3$ is higher compared to the C–H…F hydrogen bonded complexes of TFE-$CHCl_3$ mixture. Hence, the dipole of the probe molecule is not capable to perturb the C–H…O hydrogen bond present in $CHCl_3$ mixtures with ETH and MFE causing the synergetic effect of different probes in these respective mixtures. This argument is also corroborated by as the synergetic effect being less pronounced in the case of C343 as compared to C6H, C480 and C153 due to the fact that the dipole moment of C343 (9.9D) is higher as compared to the C6H (4.4 D), C480 (6.3 D) and C153 (6.6 D).[41,42] In the case of TFE-$CHCl_3$ binary mixture, the dipole of the probe probably disturb the weak C–H…F hydrogen bond between the TFE and $CHCl_3$ and get solvated more by the TFE causing preferential solvation.

Solvent Exchange Model

Solvation model developed by the Skwierczynski and Connors has been successfully applied to understand the solvation properties of many binary as well as ternary mixtures.[6,7] The solvation properties (in this case, E_T) rely on solute-solvent and solvent-solvent interactions. Selective solvent enhancement in the solvation shell of the solute takes place in the case of preferential solvation whereas, in the synergetic case, the mixed solvents adopt a different structure as compared to the each constituent due to the extensive intermolecular interaction. We have used the model developed by the Skwierczyn-

Table 2. The preferential solvation index (PSI) of alcohol over $CHCl_3$ ($\phi_{A/C}$), alcohol-$CHCl_3$ complex over $CHCl_3$ ($\phi_{CA/C}$) or ($\phi_{C_2A/C}$), alcohol-$CHCl_3$ complex over alcohol ($\phi_{CA/A}$) or ($\phi_{C_2A/A}$), the E_T value of the intermediate species (E_{TC_2A}) or (E_{TCA}) in kcal/mole, and R^2 value showing the reliability of the fitting for the $CHCl_3$ mixtures with ETH, MFE and TFE, respectively.

Model 1	$\phi_{A/C}$	$\phi_{C_2A/C}$	$\phi_{C_2A/A}$	E_{TC_2A}	R^2
$CHCl_3$-ETH	0.10	1.37	13.70	71.60	0.97
$CHCl_3$-MFE	0.09	1.06	11.77	71.45	0.97
$CHCl_3$-TFE	3.01	2.23	0.74	70.00	0.97
Model 2					
$CHCl_3$-ETH	0.44	1.34	3.04	71.33	0.99
$CHCl_3$-MFE	0.38	1.05	2.76	71.25	0.98
$CHCl_3$-TFE	18.08	12.83	0.71	71.00	0.99

ski and Connors as well as another modified model[11] to understand the solvation behavior of the $CHCl_3$ mixtures with alcohols in the solvation shell of C6H dye.

Model 1

In this model, it is assumed that $CHCl_3$ (C) and alcohol (A) interact to form a common structure CA. The solute is denoted by D. For the simplicity, it is assumed that the mixed structure of the solvent (CA) contains the solvents (C and A) in 1:1 ratio. The number of solvent molecules in the microsphere of the solvation of the solute molecule affecting its transition energy is shown by m. The solvent exchange processes are described in the eqn. (8) and (9) as follow

$$D(C)_m + m(A) \rightleftharpoons D(A)_m + m(C) \tag{8}$$

$$D(C)_m + \frac{m}{2}(A) \rightleftharpoons D(CA)_m + \frac{m}{2}(C) \tag{9}$$

E_T value of the binary mixture can be written by eqn. (10). (χ_C^S), (χ_A^S) represents the mole fraction of $CHCl_3$ and alcohol in the microsphere of the solvation of solute whereas E_{TC} and E_{TA} denote the transition energies of the solute in the pure $CHCl_3$ and alcohols, respectively.

$$E_T = \frac{(\chi_C^S \times E_{TC}) + (\chi_A^S \times E_{TA})}{(\chi_C^S + \chi_A^S)} \tag{10}$$

The preferential solvation index (PSI) of alcohol over $CHCl_3$ ($\phi_{A/C}$) and solvent mixture (CA) over $CHCl_3$ ($\phi_{CA/C}$) are given by eqn. (11) and (12). Here, χ_A^B and χ_C^B denote the mole fraction of alcohol and $CHCl_3$ in their bulk solutions.

$$\phi_{A/C} = \left(\frac{\chi_A^S}{\chi_C^S}\right) / \left(\frac{\chi_A^B}{\chi_C^B}\right)^m \tag{11}$$

$$\phi_{CA/C} = \left(\frac{\chi_{CA}^S}{\chi_C^S}\right) / \left(\frac{\chi_{CA}^B}{\chi_C^B}\right)^{m/2} \tag{12}$$

After putting PSIs in the eqn. (10) and rearranging subsequently we get

$$E_T = E_{TA} + \frac{\varsigma_1 \times (\chi_A^B)^m + \varsigma_2 \times [(1-\chi_A^B) \times \chi_A^B]^{m/2}}{(1-\chi_A^B)^m + \phi_{A/C} \times (\chi_A^B)^m + \phi_{CA/C} \times [(1-\chi_A^B) \times \chi_A^B]^{m/2}} \tag{13}$$

$$\varsigma_1 = \phi_{A/C} \times (E_{TA} - E_{TC})$$

$$\varsigma_2 = \phi_{CA/C} \times (E_{TAC} - E_{TC})$$

Model 2

In this model we have considered that alcohol and $CHCl_3$ molecules are interacting in 1:2 ratio as evident from the NMR studies and form C_2A type hydrogen bonded aggregates in the microsphere of the solvation of the solute (D). The possible solvent exchange processes are described in the eqn. (14) and (15).[11]

$$D(C)_{3m} + 3m(A) \leftrightarrows D(A)_{3m} + 3m(C) \tag{14}$$

$$D(C)_{3m} + m(A) \leftrightarrows D(C_2A)_m + m(C) \tag{15}$$

The PSI of alcohol over $CHCl_3$ ($\phi_{A/C}$) and C_2A complex over $CHCl_3$ ($\phi_{C_2A/C}$) are given by eqn. (16) and (17).

$$\phi_{A/C} = \frac{\chi_A^S/\chi_C^S}{(\chi_A^B/\chi_C^B)^{3m}} \tag{16}$$

$$\phi_{C_2A/C} = \frac{\chi_{C_2A}^S/\chi_C^S}{(\chi_{C_2A}^B/\chi_C^B)^m} \tag{17}$$

If we put eqn. (16) and (17) in the eqn. (10) and rearrange them accordingly we will get eqn. (18)

$$E_T = E_{TC} + \frac{\alpha \times (\chi_A^B)^{3m} + (E_{TC_2A} - E_{TC}) \times \phi_{C_2A/C} \times (\chi_A^B)^m \times (1-\chi_A^B)^{2m}}{(1-\chi_A^B)^{3m} + \phi_{A/C} * (\chi_A^B)^{3m} \times \phi_{C_2A/C} \times (\chi_A^B)^m \times (1-\chi_A^B)^{2m}} \tag{18}$$

$$\alpha = (E_{TA} - E_{TC}) * \phi_{A/C}$$

(Figure 6) It can be seen that the both models provide satisfactory fit to the experimental data. Both models show that PSI of complex over $CHCl_3$ or alcohol is higher as compared to the PSI of alcohol over $CHCl_3$ for the $CHCl_3$ mixtures of MFE and ETH whereas, for the $CHCl_3$ mixtures of TFE, the PSI of alcohol

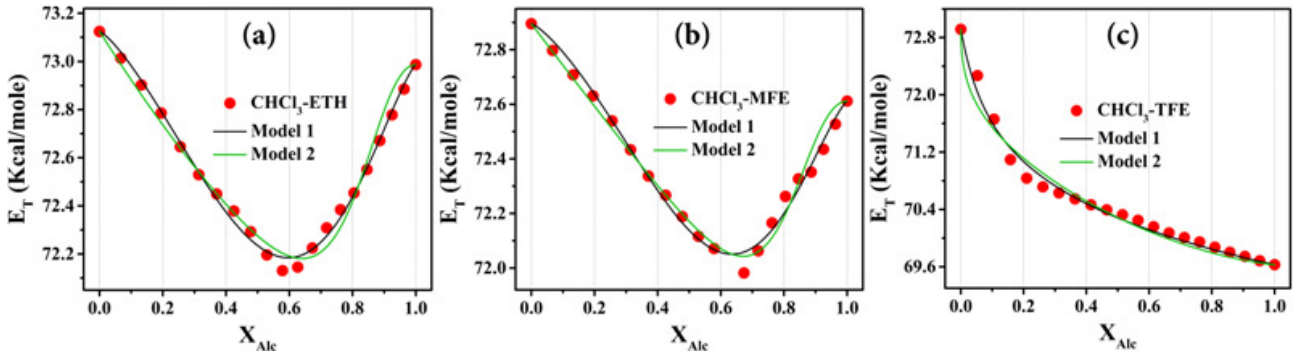

Figure 6. The fitting of E_T (kcal/mole) (experimental data in red) versus mole fraction of alcohol as well as their fitting using model 1 (black line), model 2 (green line) at different compositions of alcohols for the binary mixtures of $CHCl_3$ with ETH, MFE and TFE, respectively.

over $CHCl_3$ is higher as compared to the PSI of complex over $CHCl_3$ or alcohol. This clearly indicates that the C6H is more solvated by the complex for the $CHCl_3$ mixtures of MFE and ETH, hence, shows the synergistic effects whereas, in the case of $CHCl_3$ mixture of TFE, C6H is preferentially solvate by the TFE as the $\phi_{A/C}$ value is greater than one.

Conclusion

We have studied the behavior of binary mixtures of $CHCl_3$ with ETH, MFE and TFE using UV-Vis, NMR, IR and computational tools. The UV-Vis studies with different types of solvatochromic probes depict that molar transition energy for the binary mixtures of $CHCl_3$ with ETH and MFE are higher as compared to the bulk, whereas, for the TFE-$CHCl_3$ mixtures, it is the reverse, i.e. molar transition energy of the bulk is higher as compared to the mixture. This depicts that the $CHCl_3$ mixtures with ETH and MFE shows synergetic effect, whereas, the TFE-$CHCl_3$ mixture shows preferential solvation. NMR, IR as well as theoretical calculation establishes that the $CHCl_3$ forms the C–H…O hydrogen bonded clusters with ETH and MFE, whereas, TFE-$CHCl_3$ binary mixture are connected mainly through C–H…F hydrogen bond. The comparatively stronger C–H…O hydrogen bond in the $CHCl_3$ binary mixtures with ETH and MFE do not get perturbed by the dipole of the probe molecules, hence, showing the synergetic effect in these two binary mixtures. In contrast to the $CHCl_3$ mixtures with ETH and MFE, the binary mixture of TFE with $CHCl_3$ are connected mainly through C–H…F hydrogen bond which is weak as compared to the C–H…O hydrogen bond and gets easily perturbed by the dipole of probe molecules causing to the preferential solvation behavior for TFE-$CHCl_3$ mixture. These studies clearly illustrate that subtle change in the hydrogen bonding environment causes drastic change in the properties of solvent mixtures.

Supporting Information

The UV-Vis spectra for all the dyes, NMR spectra for the C–H of $CHCl_3$ and O–H of alcohols as well as the fluorine NMR, C–H stretching frequency of $CHCl_3$ for the different binary mixtures of $CHCl_3$ with alcohols, fitting of the model used for the NMR data along. Detailed information about the experimental section is provided in the supporting information.

Acknowledgement

This work is supported partially by the research grant provided by the Council of Scientific and Industrial Research [Grant No. 01(2803)/14/EMR-II] India as well as Department of Science and Technology, India [Grant No. EMR/2015/001605]. B.B. thanks CSIR for the fellowship.

Keywords: Alcohols · Chloroform · Solvent mixture · Hydrogen bond · Quantum chemical calculation

[1] G. M. Sando, K. Dahl, J. C. Owrutsky *J. Phys. Chem. B.* **2007**, *111*, 4901–4909.
[2] S. Dixit, J. Crain, W. C. K. Poon, J. L. Finney, A. K. Soper *Nature.* **2002**, *416*, 829–832.
[3] J. Catalán, C. Díaz, F. García-Blanco *J. Org. Chem.* **2000**, *65*, 9226–9229.
[4] V. Ramakrishnan, A. Sarua, M. Kuball, A. F. Abdullah *J. Raman Spectrosc.* **2009**, *40*, 921–935.
[5] P. L. Silva, E. L. Bastos, O. A. El Seoud *J. Phys. Chem. B.* **2007**, *111*, 6173–6180.
[6] E. Bosch, M. Rosés, K. Herodes, I. Koppel, I. Leito, I. Koppel, V. Taal *J. Phys. Org. Chem.* **1996**, *9*, 403–410.
[7] R. D. Skwierczynski, K. A. Connors *J. Chem. Soc., Perkin Trans. 2.* **1994**, 467–472.
[8] H. Salari, M. Khodadadi-Moghaddam, A. R. Harifi-Mood, M. R. Gholami *J. Phys. Chem. B.* **2010**, *114*, 9586–9593.
[9] P. P. Singh, B. R. Sharma, K. S. Sidhu *Can. J. Chem. Eng.* **1979**, *57*, 387–393.
[10] P. M. E. Mancini, A. Terenzani, C. Adam, L. R. Vottero *J. Phys. Org. Chem.* **1999**, *12*, 430–440.
[11] S. Gupta, S. Rafiq, M. Kundu, P. Sen *J. Phys. Chem. B.* **2012**, *116*, 1345–1355.
[12] M. Roses, C. Rafols, J. Ortega, E. Bosch *J. Chem. Soc., Perkin Trans. 2.* **1995**, 1607–1615.
[13] P. M. E. Mancini, A. Terenzani, C. Adam, A. Pérez, L. R. Vottero *J. Phys. Org. Chem.* **1999**, *12*, 207–220.
[14] P. M. Mancini, A. Terenzani, C. Adam, A. d. C. Pérez, L. R. Vottero *J. Phys. Org. Chem.* **1999**, *12*, 713–724.
[15] P. M. E. Mancini, A. Terenzani, C. Adam, L. R. Vottero *J. Phys. Org. Chem.* **1997**, *10*, 849–860.
[16] M. J. Kamlet, J. L. M. Abboud, M. H. Abraham, R. W. Taft *J. Org. Chem.* **1983**, *48*, 2877–2887.
[17] M. J. Kamlet, J. L. Abboud, R. W. Taft *J. Am. Chem. Soc.* . **1977**, *99*, 6027–6038.

[18] R. W. Taft, M. J. Kamlet *J. Am. Chem. Soc.* . **1976**, *98*, 2886–2894.
[19] M. J. Kamlet, R. W. Taft *J. Am. Chem. Soc.* . **1976**, *98*, 377–383.
[20] K. Kwak, D. E. Rosenfeld, J. K. Chung, M. D. Fayer *J. Phys. Chem. B.* **2008**, *112*, 13906–13915.
[21] K. Kwak, S. Park, M. D. Fayer *Proc. Natl. Acad. Sci. U. S. A.* **2007**, *104*, 14221–14226.
[22] R. Gratias, H. Kessler *J. Phys. Chem. B.* **1998**, *102*, 2027–2031.
[23] V. Dohnal, M. Tkadlecová *J. Phys. Chem. B.* **2002**, *106*, 12307–12310.
[24] M. Tkadlecová, J. Havlíček, V. Dohnal *Can. J. Chem. Eng.* **1995**, *73*, 1406–1411.
[25] K. Ishii, S. Takeuchi, T. Tahara *J. Chem. Phys.* **2009**, *131*, 044512.
[26] D. Stoner-Ma, A. A. Jaye, P. Matousek, M. Towrie, S. R. Meech, P. J. Tonge *J. Am. Chem. Soc.* . **2005**, *127*, 2864–2865.
[27] Y. Nagasawa, H. Miyasaka *Phys. Chem. Chem. Phys.* **2014**, *16*, 13008–13026.
[28] B. R. Gayathri, J. R. Mannekutla, S. R. Inamdar *J. Mol. Struct.* **2008**, *889*, 383–393.
[29] T. A. Scott *J. Phys. Chem.* **1946**, *50*, 406–412.
[30] S. M. Mejia, M. J. L. Mills, M. S. Shaik, F. Mondragon, P. L. A. Popelier *Phys. Chem. Chem. Phys.* **2011**, *13*, 7821–7833.
[31] O. Gereben, L. Pusztai *J. Phys.Chem. B.* **2015**, *119*, 3070–3084.
[32] M. A. S. Jalili *J. Comp. Chem.* **2010**, *31*, 286–294.
[33] D.-P. Hong, M. Hoshino, R. Kuboi, Y. Goto *J. Am. Chem. Soc.* . **1999**, *121*, 8427–8433.
[34] A. Jasanoff, A. R. Fersht *Biochemistry.* **1994**, *33*, 2129–2135.
[35] S. Mondal, A. U. Teja, P. C. Singh *J. Phys. Chem. A.* **2015**, 119, 3644–3652.
[36] B. Biswas, P. C. Singh *Phys. Chem. Chem. Phys.* **2015**, *17*, 30632–30641.
[37] S. Mondal, P. Chandra Singh *RSC Adv.* **2014**, *4*, 20752.
[38] B. J. van der Veken, W. A. Herrebout, R. Szostak, D. N. Shchepkin, Z. Havlas, P. Hobza *J. Am. Chem. Soc.* . **2001**, *123*, 12290–12293.
[39] K. R. N. Harris, P. J.; Derlacki, Z. J. *J. Chem. Soc. Faraday Trans.* **1998**, 94, 1963.
[40] R. Chitra, P. E. Smith *J. Chem. Phys.* **2001**, *114*, 426–435.
[41] R. J. Cave, E. W. Castner *J. Phys. Chem. A.* **2002**, *106*, 12117–12123.
[42] A. Ramalingam, C. Vijila *J. Mol. Liq.* **1999**, *81*, 237–244.

Submitted: August 11, 2016
Accepted: October 7, 2016